JOURNAL OF MATERIALS SCIENCE 12 (1977) 946–958

The formation of martensite in splat-quenched Fe-Mn and Fe-Ni-C alloys

Y. INOKUTI, B. CANTOR
School of Engineering and Applied Sciences, University of Sussex, Sussex, UK

A two-piston splat-quenching technique has been used to prepare splat-quenched Fe–Mn alloys with 0 to 20 wt % Mn, and splat-quenched Fe–Ni–C alloys with a nominal carbon content of 0.1 wt % and 0 to 40 wt % Ni. The resulting alloy microstructures have been investigated by a combination of optical and scanning electron microscopy, X-ray diffractometry, and microhardness testing; and the splat-quenched structures have been compared with the microstructures of similar alloys prepared by conventional solid-state quenching. In both alloy systems, splat-quenching produces a very small as-solidified austenite grain size, and a depression of the martensite transformation temperature as shown by an increased tendency to retain austenite to low temperatures. Because of the combination of a small austenite grain size and, therefore, fine scale martensite structure, splat-quenched martensitic alloys of Fe–Mn and Fe–Ni–C exhibit very high microhardness values.

1. Introduction

In a recent paper, we described some preliminary observations on the structure of splat-quenched Fe–Ni alloys containing 0 to 40 wt % Ni [1]. The martensite transformation temperature (M_s) in the splat-quenched alloys was found to be considerably depressed – by as much as ~ 200 K at 20 % Ni – when compared with the M_s temperature in conventional solid-state quenched alloys. Because of this effect, austenite was retained at room temperature by splat-quenching in alloys with considerably lower Ni contents than could be achieved by solid-state quenching. For instance, splat-quenched Fe–25 wt % Ni was completely austenitic at room temperature, whereas solid-state quenched Fe–25 wt % Ni is always fully martensitic [1–4]. A similar tendency to retain austenite by splat-quenching has been reported by Ruhl and Cohen for Fe–Ni–B and Fe–Ni–N alloys [5]. In addition, the fully martensitic splat-quenched alloys, including pure iron, showed large increases in hardness compared to the equivalent solid-state quenched alloys. Between 0 and 15 wt % Ni, the splat-quenched alloys had a constant Vickers microhardness of ~ 700 kg mm^{-2}; whereas in solid-state quenched alloys, the microhardness increased from ~ 70 kg mm^{-2} for pure iron to ~ 250 kg mm^{-2} at 25 wt % Ni.

The objective of the present investigation was to use a combination of X-ray diffractometry, optical and scanning electron metallography, and microhardness measurements, in order to determine whether effects similar to those described previously for splat-quenched Fe–Ni alloys [1], could also be obtained in splat-quenched Fe–Mn and Fe–Ni–C alloys. The Fe–Mn system was selected for investigation because of the considerable similarity between equilibrium Fe–Mn and Fe–Ni alloys [6]. The Fe–Ni–C system was selected for investigation, to determine whether the presence of a ternary interstitial solute enhanced the effects observed in splat-quenched Fe–Ni, as was suggested previously by Ruhl and Cohen [5].

2. Experimental technique

A series of Fe–Mn and Fe–Ni–C alloys was prepared from high purity iron (99.9+%), nickel (99.99+%), manganese (99.999+%), and carbon (99.9+%), by induction melting in recrystallized alumina crucibles under a dynamic argon atmos-

phere. The Fe–Mn alloy compositions were 5, 10, 15 and 20 wt % Mn; the Fe–Ni–C alloys each had a nominal carbon concentration of 0.1 wt % C, with nickel contents of 10, 15, 20, 25, 30, 35 and 40 wt % Ni. Several specimens of each alloy composition were splat-quenched by a two-piston technique described previously as a magnetic yoke piston [1, 7]. In this splat-quenching technique, each specimen of ~ 1 g was levitation melted under argon, then allowed to fall under gravity until quenched between two pistons which were accelerated magnetically. The magnetic field was supplied by discharging a condenser bank at 1000 V, with the discharge triggered photoelectrically by emission of light from the falling molten alloy droplet. The resulting splat-quenched specimens were very reproducible and consisted of uniform foils ~ 50 μm thick and 30 mm diameter. For a condenser voltage of 1000 V, comparison with other splat-quenching techniques has indicated that the effective cooling rate during solidification is ~ 10^6 K sec^{-1} in this two-piston splat-quencher [7]. Moreover, the ability to obtain a martensite transformation in pure iron [1] suggests that the cooling rate remains as high as ~ 10^5 to 10^6 K sec^{-1} even after solidification.

For comparison purposes, additional specimens of each alloy were prepared from the same induction melted ingots, by cold rolling to 0.5 mm thickness, austenitising for 60 min at 1273 K, and solid-state quenching into iced brine. Splat-quenched and solid-state quenched specimens were polished in HF(5%) + H_2O_2 solution and then etched in 2% nital for direct examination by optical microscopy, scanning electron microscopy in a Cambridge Instruments Stereoscan 2A, X-ray diffractometry using Co$K\alpha$ radiation, and microhardness testing. Some splat-quenched and solid-state quenched specimens of each alloy composition were cooled to 77 K by immersion in liquid nitorgen for 24 h, allowed to warm up to room temperature, and re-examined in the X-ray diffractometer.

3. Results

3.1. Fe–Mn alloys

Table I shows the results of X-ray diffractometer experiments on Fe–Mn alloys prepared as follows: splat-quenched to room temperature; splat-quenched to room temperature followed by cooling to 77 K for 24 h; solid-state quenched to room temperature; and solid-state quenched to room temperature followed by cooling to 77 K for 24 h. Also included are previous data for Fe–Mn alloys prepared by solid-state quenching to room temperature [8–10]. Splat-quenched alloys showed a greater tendency to retain austenite than the corresponding solid-state quenched alloys. Thus there were traces of austenite in Fe–10 wt % Mn splat-quenched to room temperature, and in splat-quenched Fe–15 wt % Mn, austenite was retained even after cooling to 77 K. The same alloy compositions showed no evidence of austenite when solid-state quenched.

Regardless of the method of preparation, the h c p ϵ-martensite was absent in alloys of Fe–5 and 10 wt % Mn, and was present in alloys with 15 and 20 wt % Mn. Although the proportion of ϵ-martensite was increased by cooling to 77 K, corresponding splat-quenched and solid-state quenched alloys contained similar quantities of ϵ-martensite. Thus, the increased retention of austenite in splat-quenched alloys compared to solid-state quenched alloys was at the expense of b c c α-martensite rather than h c p ϵ-martensite. For instance, no α-martensite was present in splat-quenced

TABLE I X-ray results for splat-quenched and solid-state quenched Fe–Mn alloys; phases in brackets were present in traces only

wt % Mn	Phases present				
	Splat-quenched	Splat-quenched + cooled to 77 K for 24 h	Solid-state quenched (present work)	Solid-state quenched [8–10]	Solid-state quenched + cooled to 77 K for 24 h
5	α	α	α	α	α
10	$\alpha + (\gamma)$	α	α	α	α
15	$\alpha + \gamma + (\epsilon)$	$\alpha + \gamma + \epsilon$	$\alpha + \epsilon$	$\alpha + \epsilon$	$\alpha + \epsilon$
20	$\gamma + (\epsilon)$	$\gamma + \epsilon$	$\alpha + \gamma + \epsilon$	$\alpha + \gamma + \epsilon$	$\alpha + \gamma + \epsilon$

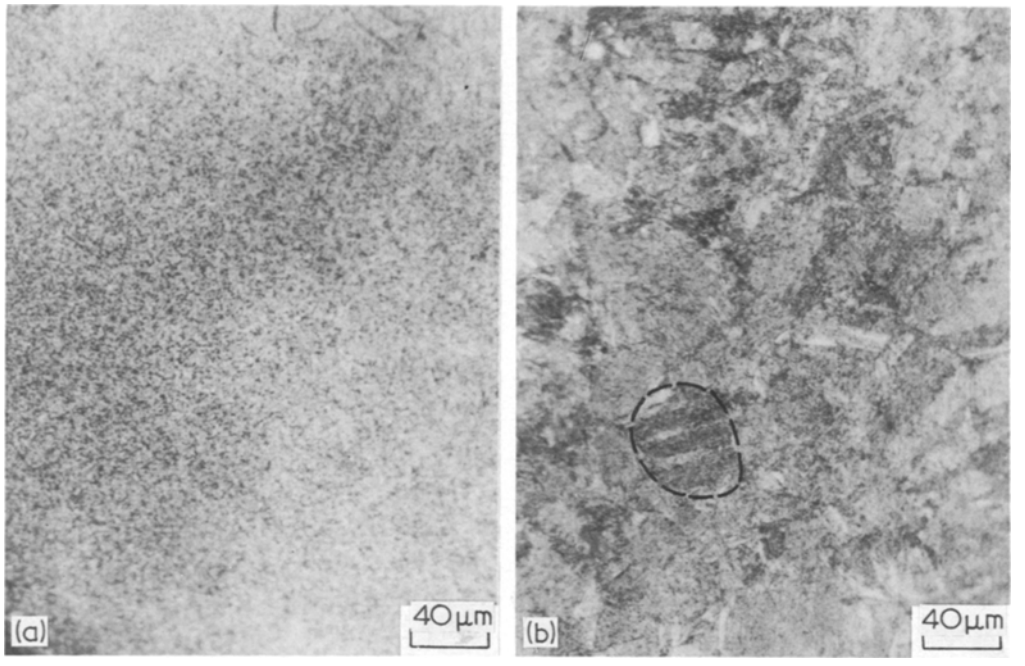

Figure 2 Optical micrographs of the surface of Fe–10 wt % Mn. (a) Splat quench; (b) solid quench.

Fe–20 wt % Mn, which consisted solely of austenite and ϵ-martensite; however, all three phases – α-martensite, austenite, and ϵ-martensite – were present in solid-state quenched Fe–20 wt % Mn.

Figs. 1 to 4 show typical optical micrographs from the surface of splat-quenched and solid-state quenched Fe–Mn alloys. The martensitic structure of the solid-state quenched alloys could be clearly resolved in the optical microscope. In solid-state quenched Fe–5 and 10 wt % Mn, the structures were typical of α-martensite (Figs. 1 and 2), whereas the ϵ-martensite in solid-state quenched

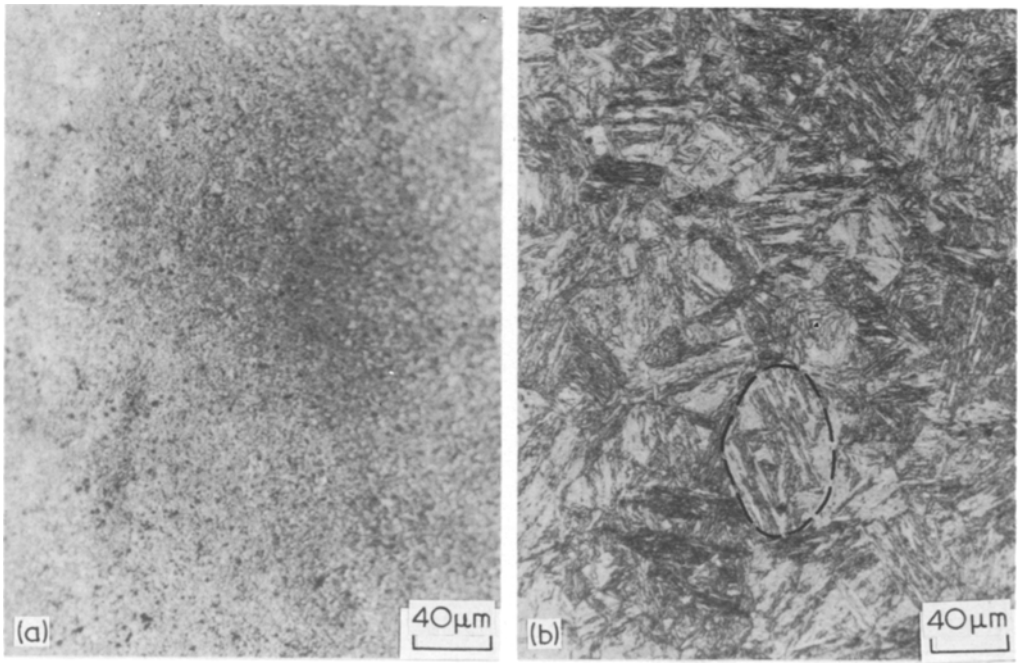

Figure 1 Optical micrographs of the surface of Fe–5 wt % Mn. (a) Splat quench; (b) solid quench.

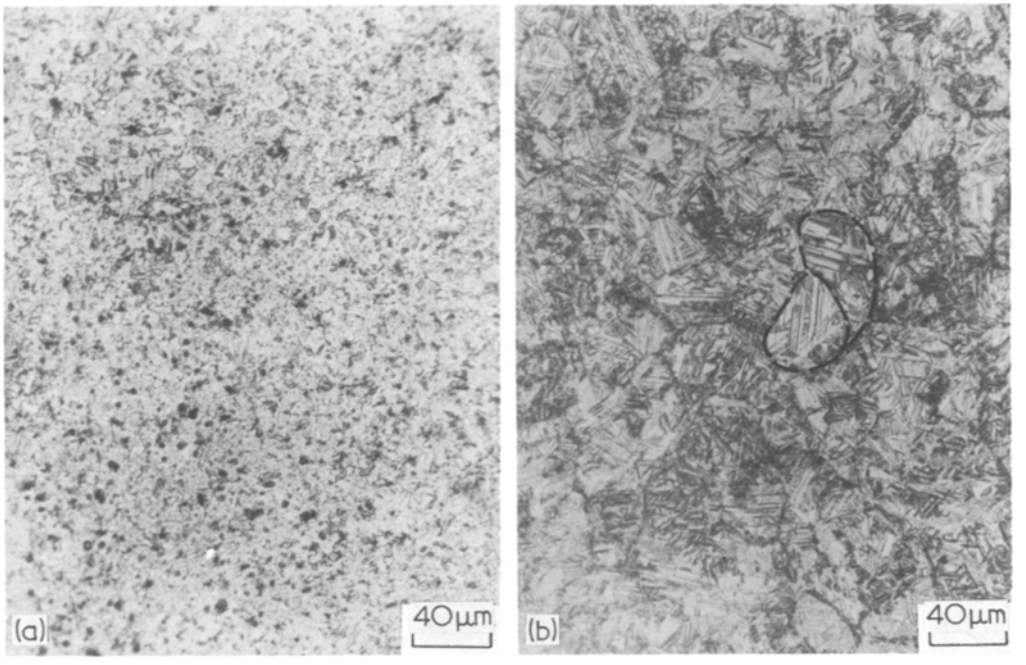

Figure 3 Optical micrographs of the surface of Fe–15 wt % Mn. (a) Splat quench; (b) solid quench.

Fe–15 and 20 wt % Mn produced a more angular morphology with sharper martensite boundaries (Figs. 3 and 4). The presence of retained austenite in solid-state quenched Fe–20 wt % Mn was evident from the incomplete martensitic morphology (Fig. 4). From the grouping of martensite plates, it was possible to infer the positions of prior austenite grain boundaries, and several examples are shown as dotted lines in Fig. 1 to 4. In this way, the prior austenite grain size was shown to be $\sim 20\,\mu m$ in all four solid-state quenched alloys. By contrast with solid-state quenched alloys, the martensitic struc-

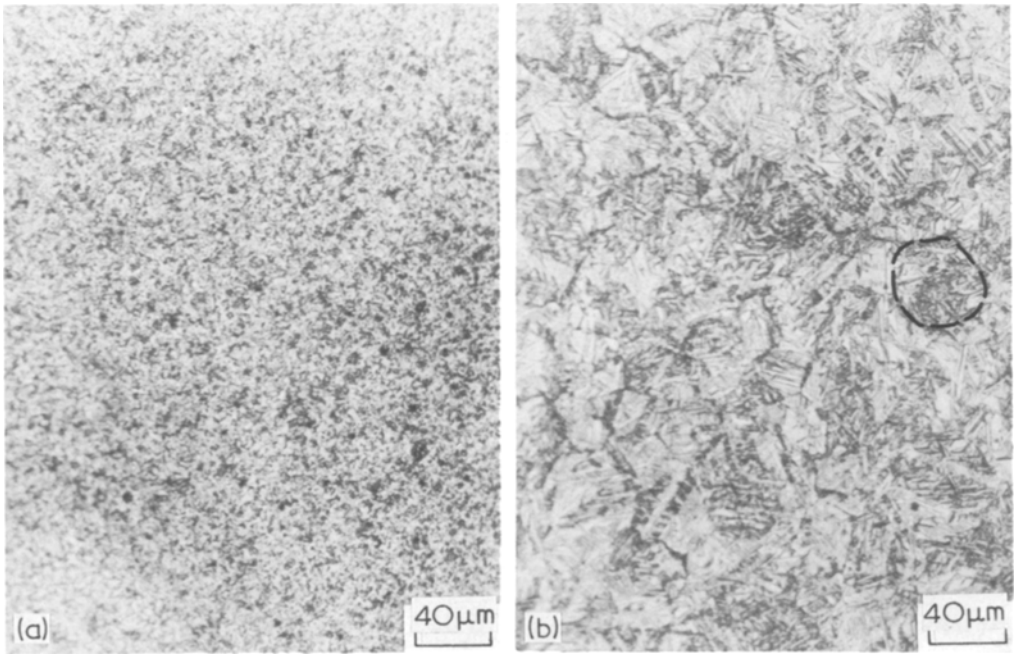

Figure 4 Optical micrographs of the surface of Fe–20 wt % Mn. (a) Splat quench; (b) solid quench.

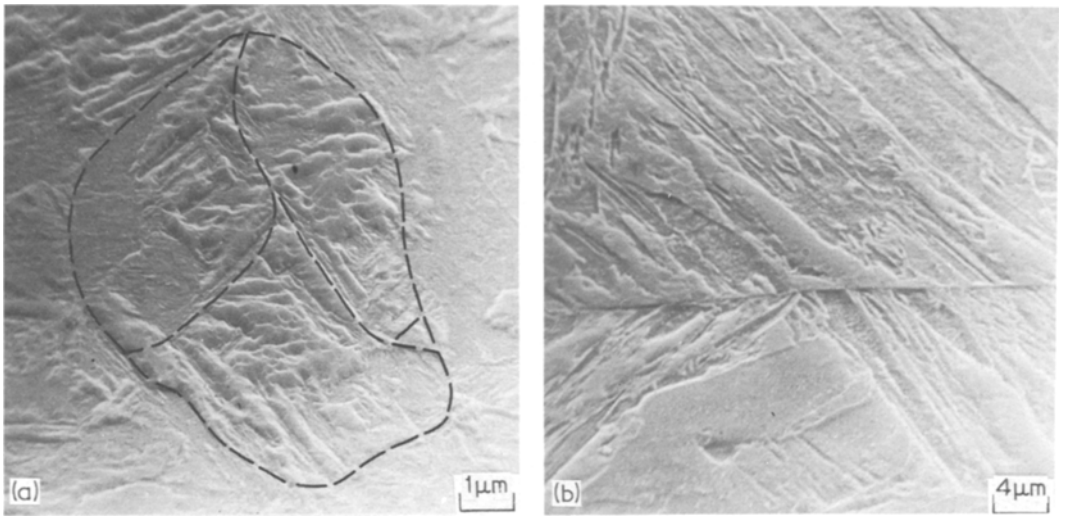

Figure 5 Scanning electron micrographs of the surface of Fe–5 wt % Mn. (a) Splat quench; (b) solid quench.

ture of splat-quenched Fe–Mn alloys was not revealed by optical metallography. All four splat-quenched alloys consisted of arrays of small grains, $\sim 5\,\mu m$ in size, which were assumed to be prior austenite grains – this interpretation was confirmed subsequently by scanning electron microscopy (Figs. 5 to 8). Thus, in both splat-quenched and solid-state quenched alloys the prior austenite grain size was independent of alloy composition, but was considerably smaller in the splat-quenched alloys. Scanning electron micrographs of cross-sections through the thickness of splat-quenched Fe–Mn alloys showed that the prior austenite grains were elongated in the solidification direction, i.e. normal to the foil surfaces, with a longitudinal grain size of $\sim 20\,\mu m$ (Fig. 9).

Figs. 5 to 8 show typical scanning electron micrographs from the surface of splat-quenched and solid-state quenched Fe–Mn alloys. The scanning electron micrographs showed very clearly the transition in solid-state quenched alloys from an α-martensite structure (Figs. 5 and 6) to a predominantly ϵ-martensite structure (Figs. 7 and 8). In addition, it was possible to resolve α-martensite in splat-quenched Fe–5 and 10 wt % Mn (Figs. 5 and 6). The splat-quenched α-martensite had an almost identical morphology to solid-state quenched α-martensite, but the martensite plates

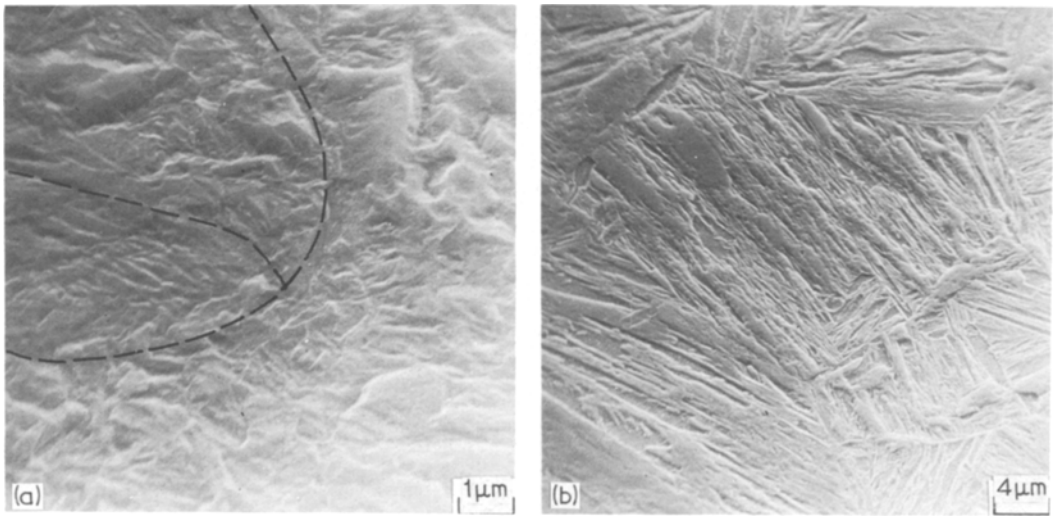

Figure 6 Scanning electron micrographs of the surface of Fe–10 wt % Mn. (a) Splat quench; (b) solid quench.

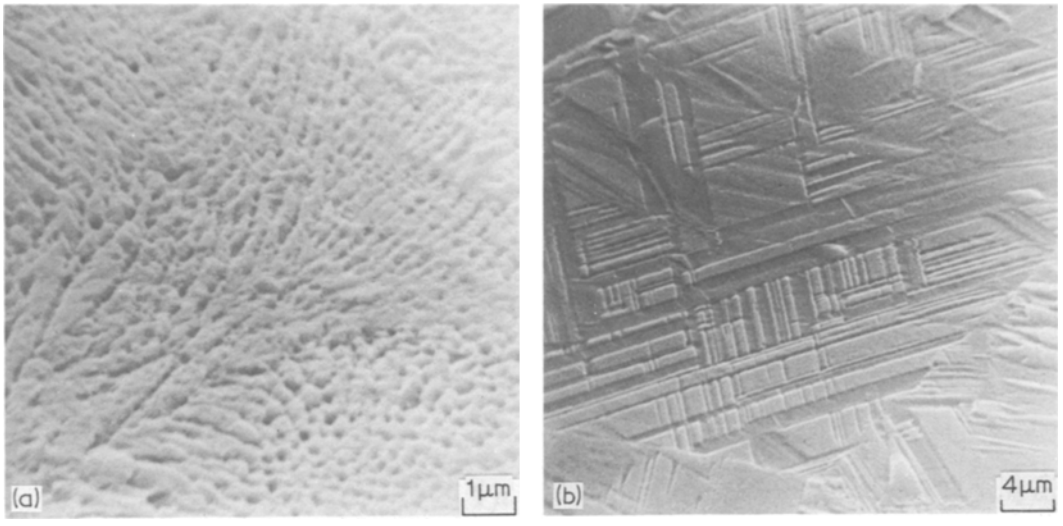

Figure 7 Scanning electron micrographs of the surface of Fe–15 wt % Mn. (a) Splat quench; (b) solid quench.

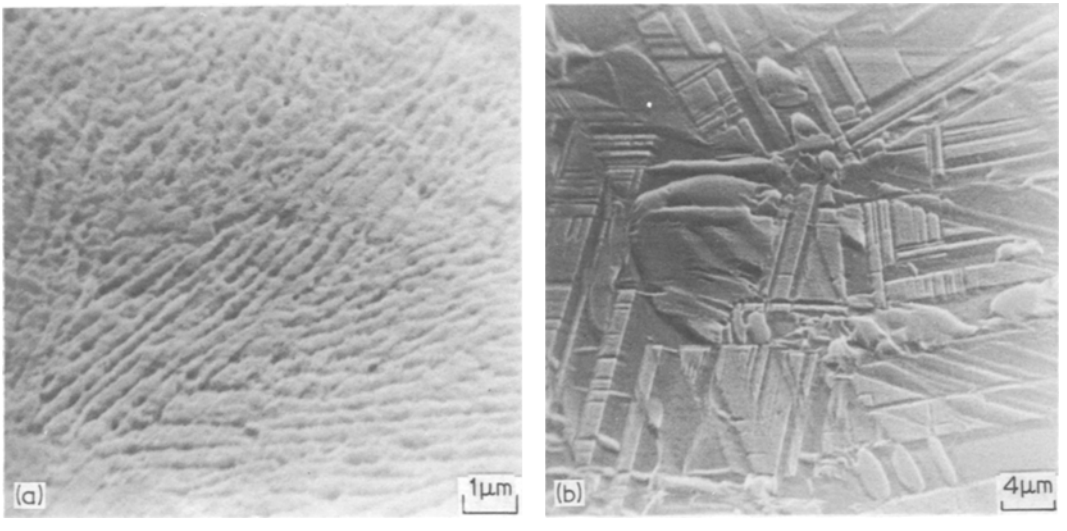

Figure 8 Scanning electron micrographs of the surface of Fe–20 wt % Mn. (a) Splat quench; (b) solid quench.

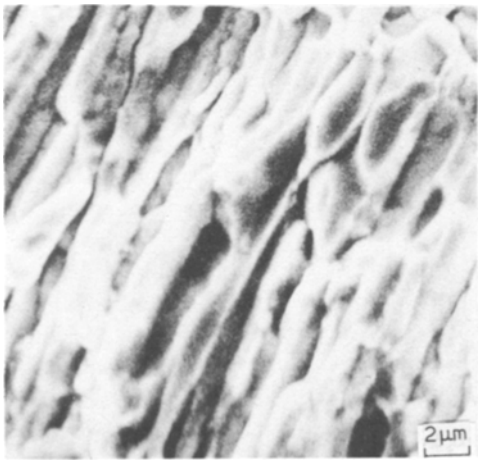

Figure 9 Scanning electron micrograph of a cross-section through the thickness of splat-quenched Fe–10 wt % Mn.

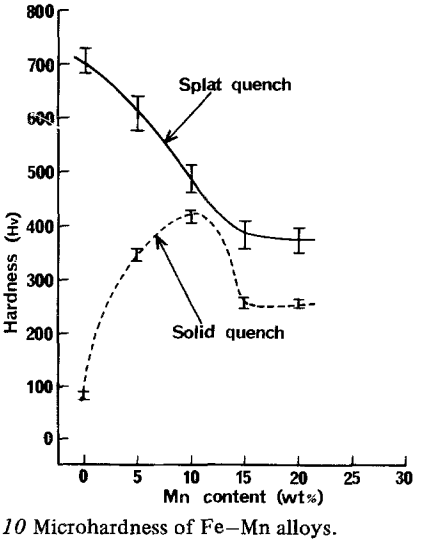

Figure 10 Microhardness of Fe–Mn alloys.

TABLE II X-ray results for splat-quenched and solid-state quenched Fe–Ni–C and Fe–Ni alloys; phases in brackets were present in traces only

wt % Ni	Phases present							
	Fe–Ni–0.1C				Fe–Ni [1–4]			
	Splat-quenched	Splat-quenched + cooled to 77 K for 24 h	Solid-state quenched	Solid-state quenched + cooled to 77 K for 24 h	Splat-quenched	Splat-quenched + cooled to 77 K for 24 h	Solid-state quenched	Solid-state + cooled to 77 K for 24 h
10	α	α	α	α	α	–	α	–
15	α	α	α	α	α	α	α	–
20	α	α	α	α	α + γ	α	α	α
25	γ	α + γ	α + (γ)	α	γ	α + γ	α	α
30	γ	α + γ	(α) + γ	α + γ	γ	α + γ	α + γ	α + γ
35	γ	γ	γ	α + γ	γ	γ	γ	α + γ
40	γ	γ	γ	γ	γ	γ	γ	γ

were about five times smaller (note the different magnifications in Figs. 5 and 6). For splat-quenched Fe–15 and 20 wt % Mn, there was no evidence of the ε-martensite, and the alloys appeared to consist of a cellular solidification morphology (Figs. 7 and 8). The ε-martensite structure was presumed to be on a finer scale, within individual solidification cells. On the scanning electron micrographs it was possible to discern the prior austenite grain boundaries in splat-quenched alloys, and an example is shown as dotted lines in Figs. 5 and 6. In this way the transverse splat-quenched prior austenite grain size was confirmed to be $\sim 5\,\mu m$, as had been inferred from optical metallography.

Fig. 10 shows the Vickers microhardness of splat-quenched and solid-state quenched Fe–Mn alloys. In solid-state quenched alloys with 0 to 10 wt % Mn, the effect of increasing Mn content was to increase the microhardness from $\sim 70\,kg\,mm^{-2}$ for pure iron to $\sim 400\,kg\,mm^{-2}$ for Fe–10 wt % Mn. At higher Mn concentrations, the formation of ε-martensite at the expense of α-martensite, and the retention of austenite (in Fe–20 wt % Mn) led to a reduction in microhardness to $\sim 250\,kg\,mm^{-2}$. In the splat-quenched alloys, increasing concentrations of Mn produced a continuous decrease in microhardness from $\sim 700\,kg\,mm^{-2}$ in pure iron to $\sim 380\,kg\,mm^{-2}$ in Fe–20 wt % Mn.

3.2. Fe–Ni–C alloys

Table II shows the structures obtained by X-ray diffractometry from splat-quenched and solid-state quenched Fe–Ni–C alloys, both as-quenched to room temperature, and after subsequent cooling to 77 K for 24 h. For comparison, previous data for splat-quenched and solid-state quenched Fe–Ni is also included [1–4]. As with the binary Fe–Ni [1] and Fe–Mn alloys, splat-quenched Fe–Ni–C showed a greater tendency to retain austenite than the corresponding solid-state quenched alloys. Thus, Fe–25 wt % Ni–0.1 wt % C was fully austenitic when splat-quenched to room temperature, but almost completely martensitic when solid-state quenched to room temperature. Similarly, no martensite was observed in splat-quenched Fe–35 wt % Ni–0.1 wt % C, whereas cooling to 77 K produced a partially martensitic structure in the same alloy when solid-state quenched. The increased tendency to retain austenite in splat-quenched Fe–Ni–C was very similar to that observed in splat-quenched Fe–Ni [1]. For instance, after cooling to 77 K, the structure of both splat-quenched and solid-state quenched alloys was independent of the presence or absence of 0.1 wt % C, so that corresponding binary and ternary alloys contained the same phases. This exact similarity was not maintained in alloys quenched to room temperature, with increased austenite content in only two Fe–Ni–C alloys (25 and 30 wt % Ni) compared to three Fe–Ni alloys (20, 25 and 30 wt % Ni).

Figs. 11 to 14 show typical optical micrographs from the surfaces of four splat-quenched and solid-state quenched Fe–Ni–C alloys. As with the Fe–Mn alloys, optical micrographs of splat-quenched Fe–Ni–C were not able to resolve the martensitic structure, but indicated a very small grain size (presumably the prior austenite grain size). In solid-state quenched Fe–Ni–C alloys, the

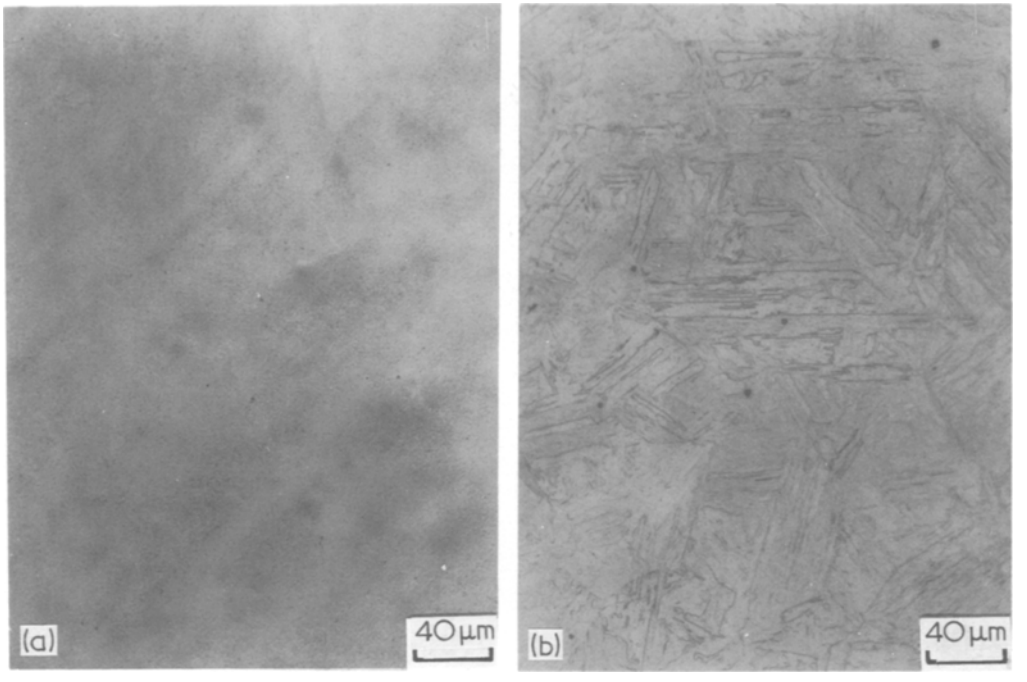

Figure 11 Optical micrographs of the surface of Fe–20 wt % Ni–0.1 wt % C. (a) Splat quench; (b) solid quench.

prior austenite grain size decreased slightly from ~ 60 μm at 20 wt % Ni to ~ 40 μm at 40 wt % Ni. The optical micrographs showed the transition in solid-state quenched Fe–Ni–C from a fully martensitic structure at 20 wt % Ni (Fig. 11), through partially martensitic structures at 25 and 30 wt % Ni (Figs. 12 and 13), to a fully austenitic structure at 40 wt % Ni (Fig. 14).

Typical scanning electron micrographs from the surfaces of splat-quenched and solid-state quenched Fe–Ni–C alloys are shown in Figs. 15 and 16. The scanning electron micrographs again showed the

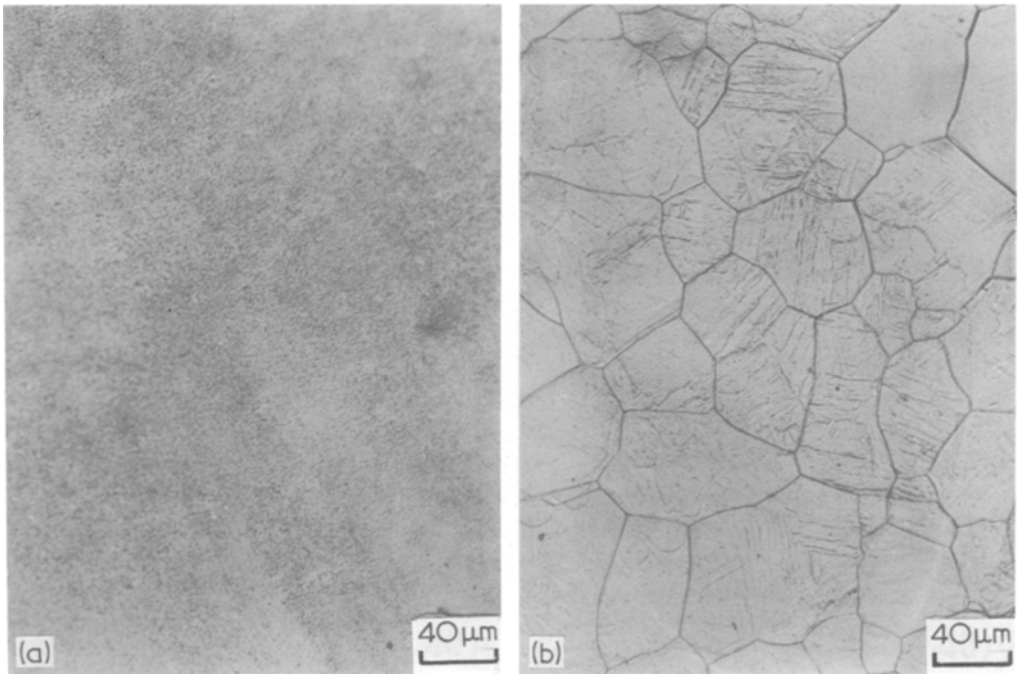

Figure 12 Optical micrographs of the surface of Fe–25 wt % Ni–0.1 wt % C. (a) Splat quench; (b) solid quench.

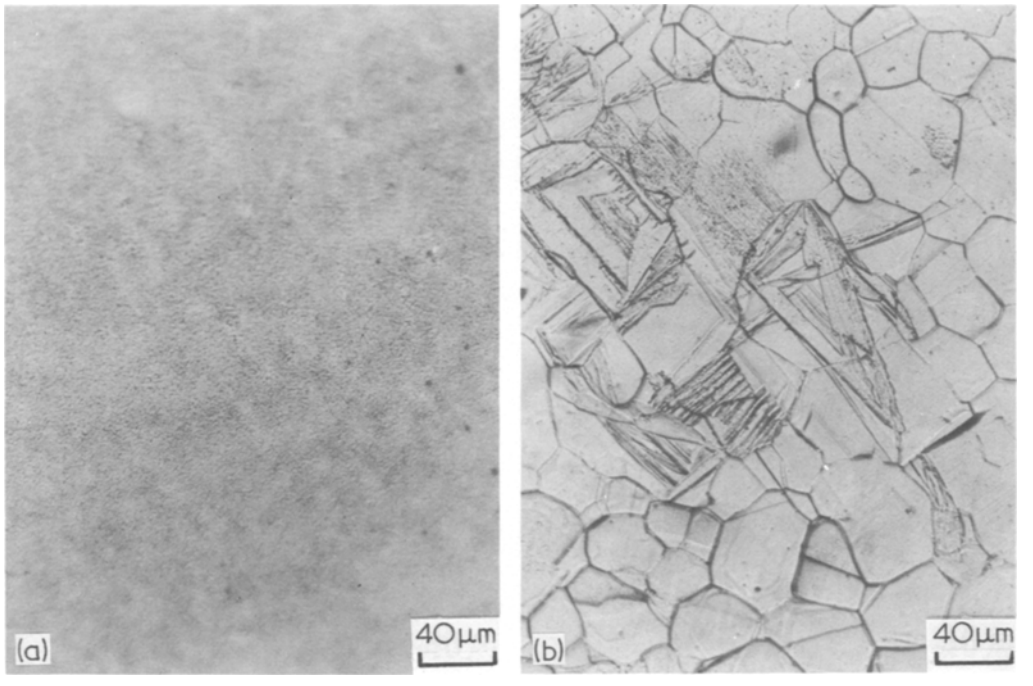

Figure 13 Optical micrographs of the surface of Fe–30 wt % Ni–0.1 wt % C. (a) Splat quench; (b) solid quench.

transition from a martensitic to an austenitic morphology with increasing Ni content in solid-state quenched Fe–Ni–C. The α-martensite structures in solid-state quenched Fe–Ni–C (Fig. 15) were remarkably similar to α-martensite in splat-quenched and solid-state quenched Fe–5 and 10 wt % Mn (Figs. 5 and 6). The scanning electron micrographs confirmed the presence of a small transverse prior austenite grain size in splat-quenched Fe–Ni–C, which was ~ 0.5 to 1.0 μm.

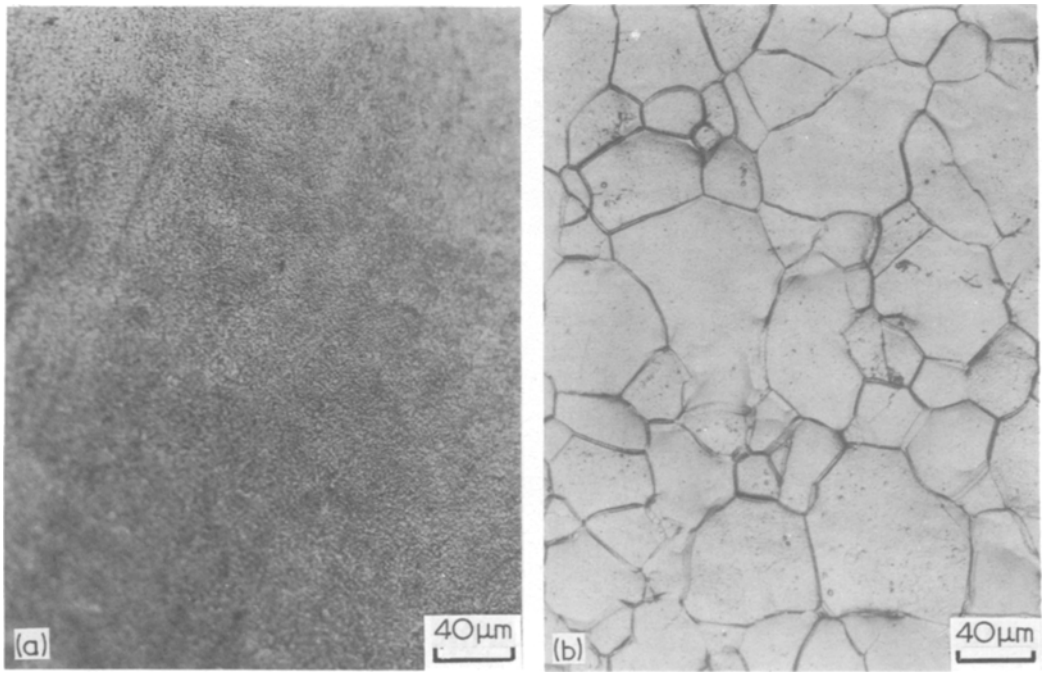

Figure 14 Optical micrographs of the surface of Fe–40 wt % Ni–0.1 wt % C. (a) Splat quench; (b) solid quench.

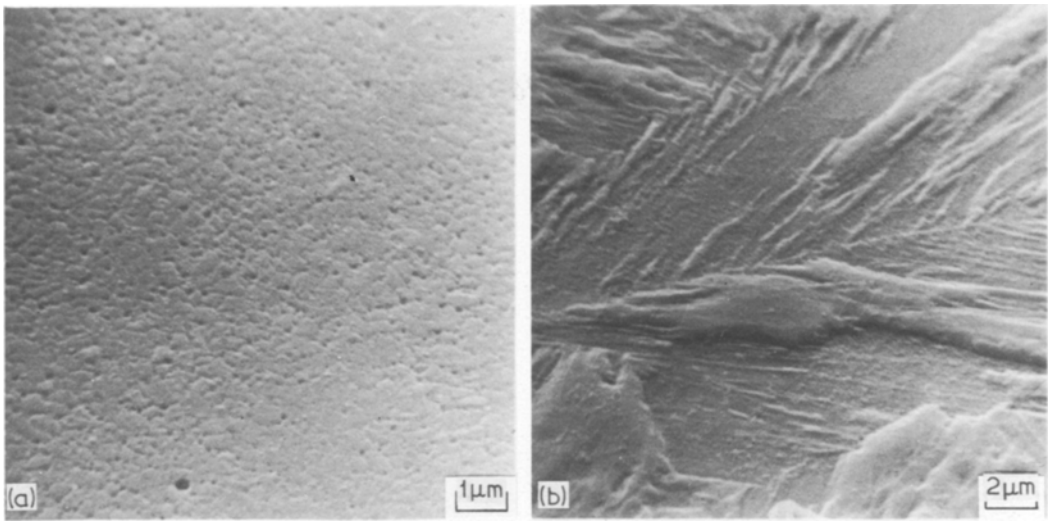

Figure 15 Scanning electron micrographs of the surface of Fe–20 wt % Ni–0.1 wt % C. (a) Splat quench; (b) solid quench.

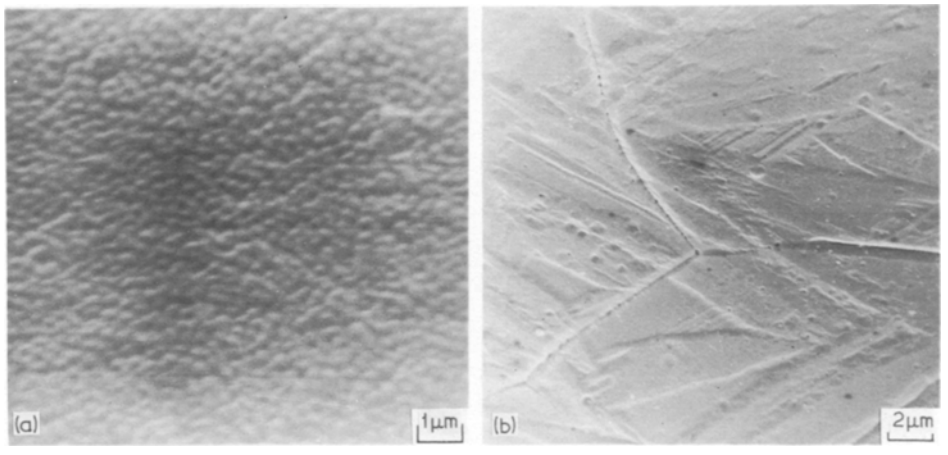

Figure 16 Scanning electron micrographs of the surface of Fe–30 wt % Ni–0.1 wt % C. (a) Splat quench; (b) solid quench.

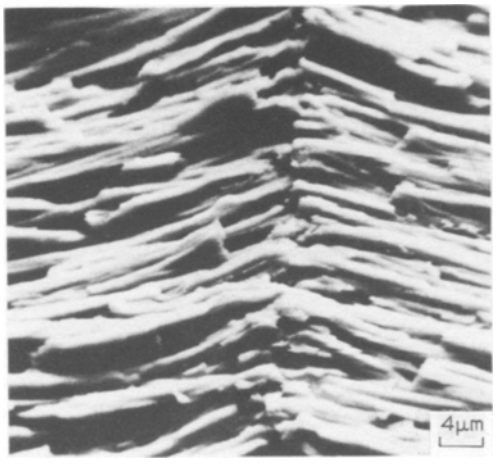

Figure 17 Scanning electron micrograph of a cross-section through the thickness of splat-quenched Fe–20 wt % Ni–0.1 wt % C.

Because of this small transverse grain size, it was not usually possible to resolve the α-martensite plates in the splat-quenched alloys (Fig. 15). Cross-sections through the thickness of splat-quenched Fe–Ni–C foils showed that the prior austenite grains were again elongated in the solidification direction, with a longitudinal grain size of ~ 20 μm (Fig. 17).

Fig. 18 shows the microhardness of Fe–Ni–C alloys as a function of Ni concentration. For comparison, the microhardness of binary Fe–Ni alloys is shown in Fig. 19. The graphs in Fig. 19 are slightly modified from those published previously [1], because more recent data have also been included [11]. For solid-state quenched specimens of both Fe–Ni–C and Fe–Ni, the microhardness increased with increasing Ni content, when the

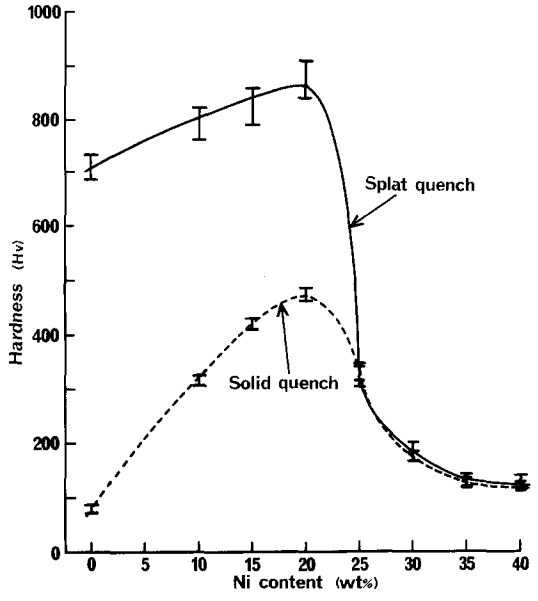

Figure 18 Microhardness of Fe–Ni–C alloys.

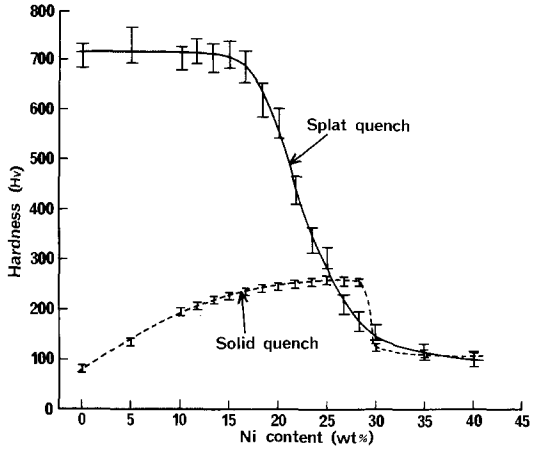

Figure 19 Microhardness of Fe–Ni alloys.

structure was fully martensitic. This increase was more pronounced in Fe–Ni–C alloys which reached a maximum microhardness of $\sim 500\,kg\,mm^{-2}$ at 20 wt % Ni, compared to $\sim 250\,kg\,mm^{-2}$ in binary Fe–20 wt % Ni. As with the previous data for splat-quenched Fe–Ni, martensitic alloys of splat-quenched Fe–Ni–C had considerably higher microhardness when compared to the equivalent solid-state quenched alloys. The effect of increasing Ni content was again to increase the microhardness of splat-quenched martensitic Fe–Ni–C to a maximum of $\sim 900\,kg\,mm^{-2}$ at 20 wt % Ni. For both binary and ternary alloys, splat-quenched and solid-state quenched, retention of austenite produced a sharp drop in the microhardness to $\sim 100\,kg\,mm^{-2}$ in fully austenitic alloys.

4. Discussion

Previous work on splat-quenched Fe–Ni [1], Fe–Ni–B [5], and Fe–Ni–N [5] alloys has shown that splat-quenching leads to an increased tendency to retain austenite compared to the equivalent alloys prepared by conventional solid-state quenching. This increased retention of austenite corresponds to a depression of the M_s temperature during splat-quenching [1]. The present results show that similar effects can also be obtained in splat-quenched Fe–Mn and Fe–Ni–C alloys. From experiments on splat-quenched Fe–Ni–B and Fe–Ni–N alloys, Ruhl and Cohen [5] have suggested that the depression of M_s is enhanced by the presence of ternary interstitial solutes. The similarity between the structures of splat-quenched Fe–Ni–0.1 wt % C and Fe–Ni alloys indicates that this is not always the case, though it is possible that a greater carbon concentration would have produced a greater depression of the M_s temperature.

The reason for the depression of the M_s temperature in splat-quenched alloys is far from clear. For specimens prepared by two-piston splat-quenching, it might be argued that a depression of M_s could be produced by magnetic fields [12], deformation [13], or hydrostatic pressure [14]. The first two of these have been rejected as possible explanations [1] because they are unlikely to produce a sufficiently large effect. Moreover, the depression of M_s in Fe–Ni–B and Fe–Ni–N prepared by gun splat-quenching [5] makes all three explanations quite unlikely, because gun splat-quenched specimens are subjected to no magnetic field, and very little deformation or hydrostatic pressure. The splat-quenched martensite is not a surface martensite [15] with different morphology, and therefore kinetics, from conventional bulk martensite. This is shown for instance by the similarity between splat-quenched and solid-state quenched α-martensite in Fe–Mn (Figs. 5 and 6).

The iced brine solid-state quench used in the present experiments produces a cooling rate well beyond the region where M_s is a function of cooling rate in solid-state quenched Fe–Mn [8]. Thus the depression of M_s in splat-quenched Fe–Mn is not caused by an insufficiently rapid cooling rate in the comparison solid-state quenched specimens.

The only possible explanation for the depression of M_s in splat-quenched alloys seems to be that it is associated with a small as-solidified austenite

grain size. A characteristic feature of all the splat-quenched alloys is a very small austenite grain size; and recent results on annealing splat-quenched Fe–Ni [11] suggest that excess retained austenite disappears when austenite grain growth takes place. Unfortunately it is very difficult to explain why a small austenite grain size should produce a depression of the M_s temperature. The kinetics of martensite transformations are believed to be controlled by the difficulty of nucleation [13], so that a smaller austenite grain size would be expected to provide more heterogeneous sites, producing a more rapid transformation and a *higher* M_s temperature.

In Fe–Ni, Fe–Mn, and Fe–Ni–C alloys, the microhardness of splat-quenched martensitic alloys is very much greater than the corresponding solid-state quenched alloys. This is presumably caused by a combination of two microstructural features; the small as-solidified austenite grain size, and the fine-scale martensite which is formed within each prior austenite grain. In Fe–Ni and Fe–Ni–C martensite, the effect of increased Ni content is similar for both splat-quenched and solid-state quenched specimens, producing a slight microhardness increase in Fe–Ni, and a considerable increase in Fe–Ni–C. However, an increasing Mn content in Fe–Mn α-martensite leads to an increased microhardness of solid-state quenched alloys, but a decreased microhardness of splat-quenched alloys. This observation suggests that splat-quenched Fe–5 wt % Mn may have been softened by traces of austenite which were undetected by X-ray diffractometry.

In all of the alloys, the presence of retained austenite produces a sharp decrease in the microhardness. In fully austenitic Fe–Ni and Fe–Ni–C, the microhardness is independent of the quenching technique and the carbon content. Thus, the small austenite grain size produced by splat-quenching high Ni alloys has almost no effect on the microhardness. This is quite different to the effect in low Ni alloys, where a small austenite grain size produces a fine-scale martensite and, therefore, very high microhardness. In high Mn alloys of Fe–Mn, the presence of ϵ-martensite maintains the splat-quenched microhardness above the value for solid-state quenched specimens.

5. Conclusions

The effect of splat-quenching Fe–Mn and Fe–Ni–C alloys is to produce a depression of the M_s temperature and an enhanced retention of austenite compared to conventional solid-state quenched alloys. For both alloy systems, splat-quenched martensitic alloys are considerably harder than the corresponding solid-state quenched alloys. Both these effects are very similar to those observed previously in splat-quenched Fe–Ni alloys [1].

Note added in proof

In order to confirm that the effects described in this paper were not caused by differences in composition between splat-quenched and solid state quenched specimens, wet chemical composition analyses were performed on alloys as-prepared (i.e. after induction melting), and after splat-quenching. The results were as given in Table III. The results showed that the process of splat-quenching led to only a very slight increase in carbon and oxygen concentrations, with other impurity concentrations unaffected. Clearly, the results presented in the paper were not caused by the pick-up of impurities during splat-quenching.

TABLE III

Alloy	%C	%N	%O	%S	%P	%Si	%Mn	%Al	%Ni
Induction melted									
Fe–5Ni–0.1C	0.115	0.003	0.004	0.003	0.003	0.008	0.002	0.002	4.90
Fe–10Ni–0.1C	0.098	0.003	0.004	0.004	0.003	0.009	0.002	0.003	10.80
Fe–15Ni–0.1C	0.097	0.003	0.004	0.003	0.003	0.009	0.002	0.003	14.75
Fe–20Ni–0.1C	0.109	0.003	0.004	0.003	0.003	0.009	0.002	0.003	20.50
Fe–10Mn	0.003	0.003	0.004	0.003	0.002	0.009	10.5	0.003	–
Fe–20Mn	0.003	0.003	0.004	0.003	0.003	0.009	21.1	0.003	–
Splat-quenched									
Fe–10Ni–0.1C	0.101	0.004	0.006	0.003	0.003	0.009	0.002	0.003	–
Fe–20Ni–0.1C	0.112	0.004	0.006	0.003	0.003	0.009	0.002	0.003	–
Fe–10Mn	0.005	0.004	0.006	0.003	0.003	0.009	10.45	0.003	–

–, not analysed.

References

1. Y. INOKUTI and B. CANTOR, *Scripta Met.* **10** (1976) 655.
2. L. KAUFMAN and M. COHEN, *Trans. Met. Soc. AIME* **206** (1956) 1393.
3. T. BELL, in "Martensite", edited by E. R. PETTY (Longman, London, 1970) Ch. 4.
4. A. GILBERT and W. S. OWEN, *Acta Met.* **10** (1962) 45.
5. R. C. RUHL and M. COHEN, *Trans. Met. Soc. AIME* **245** (1969) 253.
6. M. HANSEN and K. ANDERKO, "Constitution of Binary Alloys" (McGraw-Hill, New York, 1958).
7. R. W. CAHN, K. D. KRISHNANAND, M. LARIDJANI, M. GREENHOLZ and R. HILL, in "2nd International Conference on Rapidly Quenched Alloys", Vol. II, edited by N. J. Grant and B. C. Giessen (Elsevier, Lausanne, 1976) p.83.
8. D. W. GOMERSALL and J. GORDON PARR, *JISI* **203** (1965) 275.
9. J. D. BOLTON and E. R. PETTY, *Met. Sci. J.* **5** (1971) 166.
10. H. SCHUMANN, *Arch. Eisenhüttenw.* **38** (1967) 647.
11. Y. INOKUTI and B. CANTOR, to be published.
12. K. R. SATYANARAYAN and A. P. MIODOWNIK, in "The Mechanism of Phase Transformations in Crystalline Solids" (Inst. Metals, London, 1969) p. 162.
13. J. W. CHRISTIAN, in "Martensite", edited by E. R. PETTY (Longman, London, 1970) Ch. 2.
14. L. KAUFMAN, A. LEYENAAR and J. S. HARVEY, in "Progress in Very High Pressure Research", edited by F. P. BUNDY *et al.* (Wiley, New York, 1961) p. 90.
15. J. A. KLOSTERMANN, in "The Mechanism of Phase Transformations in Crystalline Solids" (Inst. Metals, London, 1969) p. 143.

Received 21 July and accepted 27 July 1976.